Successive-Intersection-Approximation-Based Power Flow Method for Integrated Transmission and Distribution Networks

Kunjie Tang, *Student Member, IEEE*, Shufeng Dong, and Yonghua Song, *Fellow, IEEE*

***Abstract*—This paper introduces a novel successive-intersection-approximation-based power flow method for integrated transmission and distribution networks (I-T&D). In this method, the entire I-T&D is split into the transmission network part, distribution network part, and boundary part. Then, alternate iterations are processed between a transmission network (TN) and several distribution networks (DNs) by exchanging the voltage and power injection of boundary buses. Particularly, the voltage magnitude of the boundary buses will be modified every two iterations by obtaining an intersection with the results in the previous two iterations. The local quadratic convergence of the method is proved strictly. The numerical experiment demonstrates that the proposed method has the same accuracy as the method based on the global model. Also, better convergence and efficiency can be achieved under the proposed method compared with the master-slave-splitting method in several different circumstances, DNs with loops, DNs with distributed generations, DNs with on-load tap changers, large-scale systems, etc. Besides, the proposed method is applied in the contingency analysis, achieving satisfying convergence and efficiency.**

***Index Terms*—Power flow calculation, successive intersection approximation, integrated transmission and distribution networks, distributed generations, convergence.**

I. Introduction

DUE to the rapid development of distributed generations (DGs), the coupling between transmission networks (TNs) and distribution networks (DNs) has been significantly enhanced. Under such a background, the coordinated analysis for integrated transmission and distribution networks (I-T&D) has become a hotspot in both research and real-world application [1]. Particularly, some research achievements have been achieved in the power flow of I-T&D [2]– [5], optimization and dispatch of I-T&D [5]– [8], voltage stability of I-T&D [9], coordinated restoration of I-T&D [10], [11], TN contingency analysis considering the influences of DNs [12], [13], etc. Ref. [14] systematically summarizes the models and algorithms of I-T&D analysis based on the Generalized Master-Slave Splitting Theory, which establishes an important foundation for the further research on I-T&D analysis. Among I-T&D analysis, the power flow of I-T&D is the backbone.

Under the traditional management, the equivalent model is applied, where DNs are equivalent as loads when calculating power flow of TN while TN is equivalent as a power source when calculating the power flow of DNs [2]– [4]. This model can significantly simplify the entire networks and the power flow method based on this model has high efficiency. Also, its accuracy is acceptable when limited DGs are accessed into DNs. However, with more and more DGs are accessed into DNs, the activeness of DNs has been significantly enhanced and the response of DNs towards the condition of TN has become much more complicated [2]. In this case, the simple equivalent model cannot satisfy the high accuracy requirements [2].

Theoretically, the Newton-Raphson method (NRM) based on a global model is accurate to solve the power flow of I-T&D, because the global model combines TNs and DNs as a complete network to analyze centrally without any simplification or equivalence. However, the global model is unrealistic in real-world operation due to privacy issues, numerical stability problems as well as communication burden [2], [5], [7].

Considering the inaccuracy of the equivalent model and the infeasibility of the global model, a master-slave model is proposed to describe I-T&D. Correspondingly, a master-slave-splitting-based method (MSSM) and some other similar iterative methods are proposed to calculate global power flow with alternate iterations between TNs and DNs [2]– [4]. These methods effectively overcome the disadvantages of the global model and the equivalent model [2]. TNs and DNs can be modeled heterogeneously while the overall accuracy of power flow is still maintained. However, these methods converge only when the sensitivity of reactive power injection to the voltage magnitude at the root node is small [2]. Unfortunately, with the large-scale penetration of DGs in DNs, this assumption may not hold.

To deal with the challenges discussed above, this paper applies the master-slave model and proposes a successive-intersection-approximation-based method (SIAM). The main contribution of this paper is that it

Manuscript received January 8, 2020; revised March 25, 2020 and May 5, 2020; accepted May 10, 2020. Date of publication May 14, 2020; date of current version November 4, 2020. This work was supported by National Key R&D Program of China (2016YFB0901300). Paper no. TPWRS-00036-2020. *(Corresponding author: Shufeng Dong)*

Kunjie Tang and Shufeng Dong are with the College of Electrical Engineering, Zhejiang University, Hangzhou 310027, China (e-mail: tangkunjie1994@zju.edu.cn; dongshufeng@zju.edu.cn).

Yonghua Song is with the Key Laboratory of Internet of Things for Smart City Department of Electrical and Computer Engineering University of Macau, Macau 999078, China, and also with the College of Electrical Engineering, Zhejiang University, Hangzhou 310027, China (e-mail: yhsong@um.edu.cn).

Color versions of one or more of the figures in this article are available online at https://ieeexplore.ieee.org.

Digital Object Identifier 10.1109/TPWRS.2020.2994312

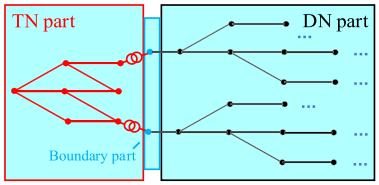

Fig. 1. Division of I-T&D.

i) introduces the general theory and specific steps of the SIAM for solving power flow of I-T&D with a rigorous convergence analysis;
ii) presents the specific method when the proposed SIAM is applied to handle loops in DNs;
iii) points out a potential weakness of the MSSM and makes a comprehensive comparison between the proposed SIAM and the MSSM in previous research both in theory and numerical experiments;

The numerical experiments demonstrate the accuracy, convergence, and the efficiency of the proposed method compared with the NRM under the equivalent model and global model, as well as the MSSM under the master-slave model.

The remaining parts of this paper are as follows. Section II presents the I-T&D power flow formulation. Section III introduces the general theory of the SIAM, including the convergence analysis and comparison with the MSSM. Section IV discusses some aspects relevant to the practical implementation of the SIAM. Numerical experiments are presented in Section V. Finally, the conclusions are drawn in Section VI.

II. I-T&D Power Flow Formulation

Real-world I-T&D usually consists of one TN and multiple DNs. Under the master-slave model, an I-T&D system is divided into the TN part, DN part, and boundary part [2], as shown in Fig. 1. The boundary part includes the boundary buses between TN and DN, i.e., the root nodes of DNs.

Thus, a model for I-T&D power flow can be formulated as:

$$\boldsymbol{G}_T(\boldsymbol{x}_T, \boldsymbol{x}_B) = \boldsymbol{0} \tag{1a}$$

$$\boldsymbol{G}_B^P(\boldsymbol{x}_T, \boldsymbol{x}_B) = \boldsymbol{P}_B \tag{1b}$$

$$\boldsymbol{G}_B^Q(\boldsymbol{x}_T, \boldsymbol{x}_B) = \boldsymbol{Q}_B \tag{1c}$$

$$\boldsymbol{G}_D(\boldsymbol{x}_D, \boldsymbol{x}_B) = \boldsymbol{0} \tag{2}$$

where the subscripts T, B, and D represent the TN part, boundary part, and DN part, respectively. The superscripts P and Q represent active power and reactive power, respectively. $\boldsymbol{x}$ represents state variables, including voltage magnitude $\boldsymbol{V}$ and angle θ under polar coordinates. Thus, (1a) represents the power flow equations in the TN part; (1b) and (1c) represent the power flow equations in the boundary part; (2) represents the power flow equations in the DN part. Under the master-slave model, the coupling between TNs and DNs is described as (1b), (1c), and $\boldsymbol{x}_B$. Here, $\boldsymbol{P}_B$ and $\boldsymbol{Q}_B$ represent power injections at the boundary buses, which are intermediate variables, independent from TN part, defined as (3)

$$\boldsymbol{P}_B = \boldsymbol{G}_{DB}^P(\boldsymbol{x}_B, \boldsymbol{x}_D) \tag{3a}$$

$$\boldsymbol{Q}_B = \boldsymbol{G}_{DB}^Q(\boldsymbol{x}_B, \boldsymbol{x}_D) \tag{3b}$$

where, $\boldsymbol{G}_{DB}^P$ and $\boldsymbol{G}_{DB}^Q$are mappings from state variables to active and reactive power injections at the boundary buses.

Here, the detailed formulations of (1)-(3) are presented in Appendix A.

III. SIAM for Solving Power Flow of I-T&D

A. Weaknesses of the MSSM

In previous research on the power flow of I-T&D, the MSSM and some similar methods are the most common method. However, these methods have potential weaknesses.

In the MSSM or similar methods, the power flow of I-T&D will be split into a TN subproblem and a DN subproblem. In the DN subproblem, with the voltage of the root node calculated in the TN power flow, power injections at the root node can be obtained. Particularly,

$$g_D(V_B) = Q_B \tag{4}$$

where g_D is a mapping from the voltage magnitude of the root node to the reactive power injection at the root node.

On the other hand, in the TN subproblem, with the power injections at the boundary bus calculated in the DN power flow, the TN power flow can be solved to obtain the voltage of all buses. Considering the decoupled PQ properties of TN, this process can be expressed as

$$g_T(Q_B) = V_B \tag{5}$$

where g_T is a mapping from the reactive power injection at the boundary bus to the voltage magnitude of the boundary bus.

Reference [2] gives several conditions for the convergence of the MSSM. The MSSM converges only when the sensitivity of reactive power injection to the voltage magnitude at the root node is small [2]. Thus, when this sensitivity is relatively large, the convergence of the MSSM cannot be guaranteed. With the rapid development of DNs, large sensitivity will commonly appear in the following circumstances.

i) There exist loops in DNs. As analyzed in [2], loops in DNs will significantly jeopardize the convergence of the MSSM. Thus, [2] and [4] propose a modified MSSM with an equivalent method to enhance the convergence when loops exist in DNs.
ii) There exist PV-typed DGs in DNs. PQ-typed DGs in DNs output constant active power and reactive power under different root nodal voltages. However, with large penetration of DGs, PV-typed DGs will be very common in DNs. Their reactive output will vary with the root nodal voltage. Thus, the sensitivity of reactive power injection to the voltage magnitude at the root node is larger compared with that in passive DNs or DNs with only PQ-typed DGs. Previous research on the MSSM does not present effective methods to handle PV-typed DGs.

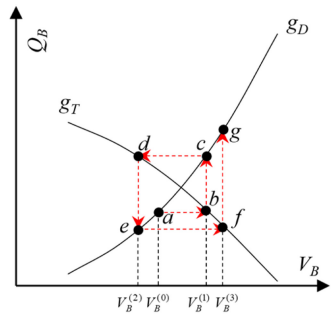

Fig. 2. The process of the MSSM.

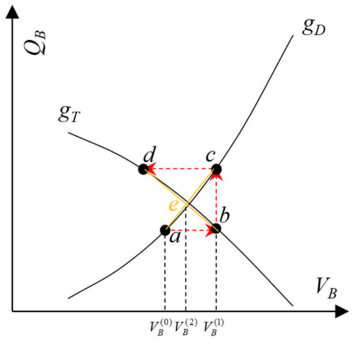

Fig. 3. The process of the SIAM.

Fig. 2 shows an example that the MSSM diverges. With alternate iterations between a TN and a DN, a series of points are achieved, a, b, …, etc. The voltage magnitude of the boundary bus varies from $V_B^{(0)}$ to $V_B^{(1)}$, $V_B^{(2)}$, … However, as shown in the figure, under the certain g_D and g_T, the MSSM will finally diverge.

B. General Theory of the SIAM

The SIAM is proposed to deal with the weakness of the MSSM. Fig. 3 shows the process of the proposed SIAM, under the same g_D and g_T presented in Fig. 2.

With alternate iterations between TN and DN, points a, b, c, and d are achieved. Instead of continuing iterations with d, as the MSSM does, the proposed SIAM needs some modifications as follows.

i) Make a line through a and c;
ii) Make another line through b and d;
iii) An intersection e is obtained. The voltage magnitude corresponding to this point will be taken as a new initial point and the TN-DN alternate iterative process is repeated.

Thus, every two TN-DN iterations, the above modification on the voltage magnitude of boundary buses will be processed with the results in the previous two iterations. A series of successive intersections gradually approach the real solution.

C. Steps of the SIAM

The proposed SIAM can be conducted as follows. For simplicity, it is assumed that one DN is connected to one TN via a boundary bus. It is not hard to generalize this method into the circumstance of multiple DNs. The numerical experiments will demonstrate the method in the circumstances of both single- and multi-DNs.

Step 1: Initialization. Set the initial value of the boundary state $\boldsymbol{x}_B^{(0)} = [\,V_B^{(0)}\ \theta_B^{(0)}\,]$. Let $\tilde{V}_B^{(0)} = V_B^{(0)}$. Set the iteration number $k = 0$ and convergence tolerance ε.

Step 2: Solve the DN part problem: solve (2) with $\boldsymbol{x}_B^{(k)}$ to obtain $\boldsymbol{x}_D^{(k+1)}$. Then, substitute $\boldsymbol{x}_B^{(k)}$ and $\boldsymbol{x}_D^{(k+1)}$ into (3) to obtain $P_B^{(k+1)}$ and $Q_B^{(k+1)}$.

Step 3: Solve the TN part problem: solve (1) with $P_B^{(k+1)}$ and $Q_B^{(k+1)}$ to obtain $\mathbf{x}_T^{(k+1)}$ and $\mathbf{x}_B^{(k+1)} = [\,V_B^{(k+1)}\ \theta_B^{(k+1)}\,]$.

Step 4: If $|\boldsymbol{x}_B^{(k+1)} - \boldsymbol{x}_B^{(k)}| < \varepsilon$, the algorithm converges and stops. Otherwise, go to *Step 5*.

Step 5: If k is an odd number: set a rectangular coordinate system, of which the x-axis represents voltage magnitude while the y-axis represents reactive power. Thus, with the results in the previous two iterations, four points $a(V_B^{(k-1)}, Q_B^{(k)})$, $b(V_B^{(k)}, Q_B^{(k)})$, $c(V_B^{(k)}, Q_B^{(k+1)})$, $d(V_B^{(k+1)}, Q_B^{(k+1)})$ are achieved. Make a line through a and c. Make another line through b and d. Calculate the x-axis coordinate of the intersection of these two lines $\tilde{V}_B^{((k+1)/2)}$ as (6)

$$\tilde{V}_B^{((k+1)/2)} = V_B^{(k-1)} - \frac{\left(V_B^{(k)} - V_B^{(k-1)}\right)^2}{V_B^{(k+1)} - 2V_B^{(k)} + V_B^{(k-1)}} \tag{6}$$

Update $V_B^{(k+1)} = \tilde{V}_B^{((k+1)/2)}$. Otherwise, if k is an even number, go to *Step 6*.

Step 6: Let $k = k + 1$. Then, go to *Step 2*.

In the SIAM, the process of *Step 2* can be expressed as

$$g_D(V_B^{(k)}) = Q_B^{(k+1)} \tag{7}$$

On the other hand, considering the decoupled PQ properties of TN, the process of *Step 3* can be expressed as

$$g_T(Q_B^{(k)}) = V_B^{(k)} \tag{8}$$

By calculating the coordinate of the intersection, it is not difficult to discover that, SIAM is an iterative method with the following recursion relation in essence

$$\tilde{V}_B^{(n+1)} = \tilde{V}_B^{(n)} - \frac{\left(\varphi(\tilde{V}_B^{(n)}) - \tilde{V}_B^{(n)}\right)^2}{\varphi(\varphi(\tilde{V}_B^{(n)})) - 2\varphi(\tilde{V}_B^{(n)}) + \tilde{V}_B^{(n)}}, \quad n = 0, 1, 2, \ldots \tag{9}$$

where

$$\varphi(\tilde{V}_B^{(n)}) = g_T(g_D(\tilde{V}_B^{(n)})) \tag{10}$$

Note that this recursion implies an iteration from n to $n+1$, which encompasses twice iterations in the MSSM. This recursion is presented for convergence analysis in Subsection D. However, an iteration of the proposed SIAM shown in numerical experiments still means that DN power flow and TN power flow are solved once respectively, which is similar to once iteration

in the MSSM. Thus, the iteration numbers of the MSSM and the proposed SIAM can be compared directly.

D. Convergence Analysis

First, the following conditions are assumed for the convergence analysis of the proposed SIAM:

i) The power flow problem has a solution. Thus, there exists a final solution $\tilde{V}_B^*$ for recursion (9), i.e., $\varphi(\tilde{V}_B^*) = \tilde{V}_B^*$;
ii) $\varphi''(\cdot)$ is continuous in a neighborhood of $\tilde{V}_B^*$, denoted as$U(\tilde{V}_B^*)$;
iii) $\varphi'(\cdot) \neq 1$ in the neighborhood $U(\tilde{V}_B^*)$.

Here, it is assumed that all these prerequisites are satisfied in the I-T&D power flow. Then, Theorem I is established.

Theorem I: Under conditions i)-iii), if the initial value $\tilde{V}_B^{(0)}$ is in a neighborhood $U(\tilde{V}_B^*)$ of $\tilde{V}_B^*$ satisfying conditions ii)-iii), the recursion (9) converges to $\tilde{V}_B^*$ with a local quadratic convergence rate.

Proof: For simplicity, let $v_n = \tilde{V}_B^{(n)}, v* = \tilde{V}_B^*$.

Rewrite (9) as

$$v_{n+1} = F(v_n) \tag{11}$$

$$F(v_n) = v_n - \frac{f(v_n)^2}{f(v_n + f(v_n)) - f(v_n)} \tag{12}$$

$$f(v_n) = \varphi(v_n) - v_n \tag{13}$$

Let

$$e_n = v_n - v* \tag{14}$$

From Taylor's expansion,

$$F(v_n) \approx F(v*) + (v_n - v*)F'(v*) + \frac{1}{2}(v_n - v*)^2 F''(v*)$$

$$= v* + e_n F'(v*) + \frac{1}{2}e_n^2 F''(v*) \tag{15}$$

So,

$$e_{n+1} = v_{n+1} - v* = F(v_n) - v* \approx e_n F'(v*) + \frac{1}{2}e_n^2 F''(v*) \tag{16}$$

Thus, it is sufficient to show $F'(v*) = 0$ to prove Theorem I.

Since $\varphi'(\cdot) \neq 1$,

$$f'(v*) = \varphi'(v*) - 1 \neq 0 \tag{17}$$

Since $f(v*) = 0$ and $f'(v*) \neq 0$,

$$\lim_{v \to v*} F(v) = v* - \lim_{v \to v*} f(v) \lim_{v \to v*} \frac{f(v)}{f(v + f(v)) - f(v)}$$

$$= v* - \frac{f(v*)}{f'(v*)} = v* \tag{18}$$

From Taylor's expansion,

$$f(v + f(v)) = f(v) + f'(v)f(v) + \frac{1}{2}f''(\xi)f(v)^2 \tag{19}$$

where ξ is between v and $v + f(v)$.

Thus,

$$\frac{f(v + f(v)) - f(v)}{f(v)} = \frac{f'(v)f(v) + \frac{1}{2}f''(\xi)f(v)^2}{f(v)}$$

$$= f'(v) + \frac{1}{2}f''(\xi)f(v) \tag{20}$$

Then,

$$F(v) = v - \frac{f(v)^2}{f(v + f(v)) - f(v)} = v - \frac{f(v)}{f'(v) + \frac{1}{2}f''(\xi)f(v)} \tag{21}$$

$$\frac{F(v) - F(v*)}{v - v*} = \frac{v - \frac{f(v)}{f'(v) + \frac{1}{2}f''(\xi)f(v)} - v*}{v - v*}$$

$$= 1 - \frac{f(v) - f(v*)}{v - v*} \frac{1}{f'(v) + \frac{1}{2}f''(\xi)f(v)} \tag{22}$$

$$F'(v*) = \lim_{v \to v*} \frac{F(v) - F(v*)}{v - v*} = 1 - f'(v*)\frac{1}{f'(v*)} = 0 \tag{23}$$

Therefore, Theorem I is established and the SIAM has a local quadratic convergence rate.

E. Advantages of SIAM

First, because the SIAM is based on the master-slave model, it has some similar advantages with the MSSM as follows

- It limits the model and data exposure compared with the methods based on the global model. Considering that TNs and DNs usually have different operational objectives and benefits, the amount of model and data sharing between them should be limited. The SIAM based on the master-slave model can guarantee this point.
- It allows a heterogeneous model to be established. The significant property difference between TNs and DNs can be handled under the SIAM model, such as the network structure, the order of magnitude of parameters, the convergence criteria, etc. The power flow in the TN part and DN part are solved separately in Step 2 and Step 3, which indicates that different modeling, different solving methods, and different convergence tolerance can be applied. For example, TN power flow can be modeled as single-phase and solved with NRM, of which the convergence tolerance is set to 1e-4 p.u., while DN power flow can be modeled as three-phase and solved with the back/forward sweep method, of which the convergence tolerance is set to 1e-6 p.u.

Meanwhile, even compared with the popular MSSM, the proposed SIAM has significant advantages.

- It has better convergence. The conditions for the convergence of the MSSM are released in the SIAM, so the SIAM has a larger region of convergence. Even when the sensitivity of reactive power injection to the voltage magnitude at the root node is relatively large, the SIAM can still converge within limited iterations.
- It has a higher convergence rate. As mentioned above, the MSSM has a local linear convergence rate [4] while the SIAM has a local quadratic convergence rate.

IV. Discussions and Extensions

A. Discussions About Unbalanced DNs

In real-world operation, the three-phase imbalance in DNs should be considered. Two methods can be used to modify the proposed algorithms and to make them accommodate three-phase systems.

First, the TN and DNs are all considered as three-phase systems. This method is direct and easy to calculate. However, it is time-consuming and does not fully exploit the characteristic of TN [2].

Ref. [2] proposes a heterogeneous model, where the TN is modeled as single-phase while DNs are modeled as three-phase. This model can be applied to extend the proposed SIAM into a three-phase form. It needs additional calculation in the boundary system [2]. In specific, for a DN, it is assumed that the three-phase voltage at its root node is symmetric in each iterative step, i.e., the $V_B^{(k)}$ and $\theta_B^{(k)}$ in the DN power flow in *Step 2* can be expressed as (24) and (25), respectively

$$V_{Ba}^{(k)} = V_{Bb}^{(k)} = V_{Bc}^{(k)} \tag{24}$$

$$\theta_{Ba}^{(k)} = \theta_{Bb}^{(k)} + \frac{2}{3}\pi = \theta_{Bc}^{(k)} + \frac{4}{3}\pi \tag{25}$$

where $V_{Ba}^{(k)}$ and $\theta_{Ba}^{(k)}$ are obtained from the single-phase TN power flow in *Step 3* in the last iteration. The subscripts *a*, *b*, and *c* represent three different phases. For the TN, the $P_B^{(k)}$ and $Q_B^{(k)}$ in the TN power flow in *Step 3* can be calculated as

$$P_B^{(k)} = P_{Ba}^{(k)} + P_{Bb}^{(k)} + P_{Bc}^{(k)} \tag{26}$$

$$Q_B^{(k)} = Q_{Ba}^{(k)} + Q_{Bb}^{(k)} + Q_{Bc}^{(k)} \tag{27}$$

where $P_{Ba}^{(k)}$, $P_{Bb}^{(k)}$, $P_{Bc}^{(k)}$, $Q_{Ba}^{(k)}$, $Q_{Bb}^{(k)}$, and $Q_{Bc}^{(k)}$ are the results in the three-phase imbalanced DN power flow in *Step 2*.

B. Discussions About DNs With Loops

When the proposed SIAM is applied to solve the power flow of DNs with loops, some measurements are required to enhance the convergence. Like [2], [5], *Step 1*-*Step 3* in Section III-C need to be modified.

Step 1': Initialization. Set the initial value of the boundary state $\boldsymbol{x}_B^{(0)} = [\, V_B^{(0)} \ \theta_B^{(0)} \,]$. Let $\tilde{V}_B^{(0)} = V_B^{(0)}$. Set the iteration number $k = 0$ and convergence tolerance ε. Form the equivalent admittance matrix of the DN $\boldsymbol{Y}_{eq}$ by reserving root nodes while eliminating all the other nodes.

Assumed that $\boldsymbol{Y}_D$ represents the original admittance matrix of the DN, n_r represents the number of feeders in this DN, and n_D represents the number of nodes in this DN. Also, without losing generality, it is assumed that Node $1 \sim n_r$ are root nodes.

$$\boldsymbol{Y}_D = \begin{bmatrix} y_{1,1} & \cdots & y_{1,n_r} & y_{1,n_r+1} & \cdots & y_{1,n_D} \\ \cdots & \cdots & \cdots & \cdots & \cdots & \cdots \\ y_{n_r,1} & \cdots & y_{n_r,n_r} & y_{n_r,n_r+1} & \cdots & y_{n_r,n_D} \\ y_{n_r+1,1} & \cdots & y_{n_r+1,n_r} & y_{n_r+1,n_r+1} & \cdots & y_{n_r+1,n_D} \\ \cdots & \cdots & \cdots & \cdots & \cdots & \cdots \\ y_{n_D,1} & \cdots & y_{n_D,n_r} & y_{n_D,n_r+1} & \cdots & y_{n_D,n_D} \end{bmatrix} \tag{28}$$

Thus, $\boldsymbol{Y}_{eq}$ is calculated as

$$\boldsymbol{Y}_{eq} = \boldsymbol{Y}_{11} - \boldsymbol{Y}_{12}\boldsymbol{Y}_{22}^{-1}\boldsymbol{Y}_{21} \tag{29}$$

where

$$\boldsymbol{Y}_{11} = \begin{bmatrix} y_{1,1} & \cdots & y_{1,n_r} \\ \cdots & \cdots & \cdots \\ y_{n_r,1} & \cdots & y_{n_r,n_r} \end{bmatrix}$$

$$\boldsymbol{Y}_{12} = \begin{bmatrix} y_{1,n_r+1} & \cdots & y_{1,n_D} \\ \cdots & \cdots & \cdots \\ y_{n_r,n_r+1} & \cdots & y_{n_r,n_D} \end{bmatrix}$$

$$\boldsymbol{Y}_{21} = \begin{bmatrix} y_{n_r+1,1} & \cdots & y_{n_r+1,n_r} \\ \cdots & \cdots & \cdots \\ y_{n_D,1} & \cdots & y_{n_D,n_r} \end{bmatrix}$$

$$\boldsymbol{Y}_{22} = \begin{bmatrix} y_{n_r+1,n_r+1} & \cdots & y_{n_r+1,n_D} \\ \cdots & \cdots & \cdots \\ y_{n_D,n_r+1} & \cdots & y_{n_D,n_D} \end{bmatrix} \tag{30}$$

Step 2': Solve the DN part problem: solve (2) with $\boldsymbol{x}_B^{(k)}$ to obtain $\boldsymbol{x}_D^{(k+1)}$. Then, substitute $\mathbf{x}_B^{(k)}$ and $\mathbf{x}_D^{(k+1)}$ into (3) to obtain $P_B^{(k+1)}$ and $Q_B^{(k+1)}$. Then, update $P_B^{(k+1)}$ and $Q_B^{(k+1)}$ with (31) and (32) considering 'virtual' power injections related to $\boldsymbol{Y}_{eq}$. The modified $P_B^{(k+1)}$ and $Q_B^{(k+1)}$ will be applied in *Step 3*'.

$$P_B^{(k+1)} \leftarrow P_B^{(k+1)} - \mathrm{Re}(diag\{\dot{\boldsymbol{U}}_B^{(k)}\}\boldsymbol{Y}_{eq}\overline{\dot{\boldsymbol{U}}}_B^{(k)}) \tag{31}$$

$$Q_B^{(k+1)} \leftarrow Q_B^{(k+1)} - \mathrm{Im}(diag\{\dot{\boldsymbol{U}}_B^{(k)}\}\boldsymbol{Y}_{eq}\overline{\dot{\boldsymbol{U}}}_B^{(k)}) \tag{32}$$

where

$$\dot{U}_B^{(k)} = V_B^{(k)}\cos\theta_B^{(k)} + jV_B^{(k)}\sin\theta_B^{(k)} \tag{33}$$

Step 3': Solve the TN part problem: solve modified (1) with $P_B^{(k+1)}$ and $Q_B^{(k+1)}$ to obtain $\mathbf{x}_T^{(k+1)}$ and $\mathbf{x}_B^{(k+1)}$. Here, in the modified (1), the equivalent admittance matrix of the DN $\boldsymbol{Y}_{eq}$ needs to be added into the admittance matrix of the TN $\boldsymbol{Y}_T$ with (34)

$$\boldsymbol{Y}_T(\sigma(i),\sigma(j)) \leftarrow \boldsymbol{Y}_T(\sigma(i),\sigma(j)) + \boldsymbol{Y}_{eq}(i,j), 1 \le i,j \le n_r \tag{34}$$

where $\sigma(i)$ represents the bus number of the bus in the TN which is connected to Node *i* in the DN.

The accuracy of the above steps is demonstrated in Appendix B in [5]. Also, [5], [14] explain the theory underlying this improvement with mathematical analysis. From a generalized perspective, as shown in the references, the equivalence of DNs establishes a 'distribution-response function' and a new decomposition is constructed based on this function. It can be demonstrated that the new decomposition will make the TN-DN power flow methods converge faster from a sensitivity analysis or a spectral radius analysis perspective [5], [14].

C. Discussions About DGs With Volt-Var Control

In Section III, loops and PV-typed DGs in DNs are analyzed. These two factors may enlarge the sensitivity of reactive power injection to the voltage magnitude at the root node. Further, they lead to a low convergence rate or even divergence of

the conventional MSSM. Here, the sensitivity of active power injection to the voltage magnitude at the root node is not fully considered, because this sensitivity is relatively small without volt-var control.

However, with the advancement of various smart inverters, DGs with volt-var control should be also considered. When DGs with volt-var control exist in DNs, their active power output will vary with the root nodal voltage. Thus, the sensitivity of active power injection to the voltage magnitude at the root node may be larger compared with that in passive DNs or DNs with only PQ-typed DGs. When this sensitivity is large, the convergence of the conventional MSSM will be also declined. The numerical experiments demonstrate that the proposed SIAM with V-Q iterations can also significantly improve the convergence in this circumstance.

D. Discussions About On-Load Tap Changers

When on-load tap changing transformers exist in DNs, their ratios will influence the sensitivity of reactive power injection to the voltage magnitude at the root node, and further influence the overall performance of I-T&D power flow methods. Also, the ratios of transformers at TN-DN boundaries will influence the sensitivity of the voltage magnitude to the reactive power injection at the boundary buses in TN power flow subproblems. This may also influence the overall performance.

On the other hand, the on-load tap changing transformer is usually equipped with an automatic voltage regulator to control voltage through actions of an on-load tap changer. Without losing generality, it is assumed that tap changers control voltage by single-criterion, i.e., one tap changer constrains the voltage magnitude of one node when the voltage of this node violates its limit. To consider the action of tap changers, after calculating the power flow, the voltage limits of the nodes constrained by tap changers need to be checked. The tap changers should change their positions if the corresponding nodes violate voltage limits. After that, power flow is recalculated. This process is repeated until the voltage magnitudes of all the nodes constrained by tap changers are kept within the allowed voltage intervals. As mentioned before, different ratios of tap changers may influence the overall performance. Also, several rounds of power flow calculation lead to cumulative effects and make a higher requirement on the performance of I-T&D power flow methods.

Numerical experiments demonstrate that the proposed SIAM show stable convergence and efficiency when handling on-load tap changers and their action.

E. Discussions About Selection of Iteration Variables

In DN power flow calculation, the root nodal voltage V affects both active and reactive power injections (P and Q), at the root node in DNs, not only reactive power injection. However, only V-Q iteration is considered as shown in (3) and (4) in Section III-A. The selection of iteration variables can be attributed to the following reasons:

i) In DN parts, active and reactive power injections are achieved simultaneously in pairs given a root nodal voltage. Thus, replacing (P, Q) with Q can still partly describe the characteristics of the power flow distribution in DN parts. Admittedly, when DGs in DN parts are considered, g_D may not be a monotone function and different root nodal voltages may correspond to the same Q. In this case, Q cannot uniquely represent a power flow distribution of DN without P. But, considering that the convergence of I-T&D power flow requires the boundary matching of voltage, the validity of the final solutions is guaranteed.
ii) In the TN part, P and Q can be decoupled approximately-active power distribution is mainly influenced by voltage angle while reactive power distribution is mainly influenced by voltage magnitude. In other words, in TN power flow, the sensitivity of the voltage magnitude of a boundary bus to active power injection at this bus is much smaller than that to reactive power injection. Thus, in TN power flow results, the voltage magnitude of the boundary bus V is mainly determined by the reactive power injection Q at the boundary bus. Combined with the reason (i), replacing (P, Q) with Q in iterations is reasonable.
iii) Compared with V-(P, Q) iteration, V-Q iteration is simpler and easier to implement because only the value of reactive power injection needs to be updated every two iterations.

In summary, reducing V-(P, Q) iteration to V-Q iteration can still guarantee the validity of final solutions and achieve satisfying convergence. Considering that the convergence criteria are satisfied in both TN and DN parts, and the TN-DN boundary matching of voltage and power injections are guaranteed, the final solutions are correct. Also, numerical experiments in Section V demonstrates that applying V-Q iteration can achieve satisfying convergence and efficiency.

F. Application in Contingency Analysis

The proposed SIAM is applicable in contingency analysis. Some researchers have obtained important achievements in TN contingency analysis considering the influences of DNs [12], [13]. As presented in [12], in TN contingency analysis, I-T&D power flow is calculated under each contingency. Ref. [12] applies the MSSM for power flow calculation, so it may suffer from a low convergence rate or even divergence, as mentioned above. Thus, the proposed SIAM can be applied in contingency analysis to improve convergence and efficiency.

Some contingency screening strategies are proposed in [12], [13]. These strategies can also be used to accelerate SIAM-based contingency analysis. However, considering that this paper mainly focuses on the power flow method, these strategies will not be discussed specifically.

V. Numerical Experiment

The programs for the test run on the Windows 10 of 64 bits. The CPU is Intel Core i7-7700K, with 4.20GHz master frequency and 32GB memory. The programming language used is MATLAB R2019a. The convergence tolerance of power flow methods is set to 1e-6 p.u. Several I-T&D cases are constructed

TABLE I
POWER FLOW RESULTS OF THE BOUNDARY PART

Case	Data	Bus No.	NRM-GM	NRM-EM	MSSM	SIAM
A1	V_B /p.u.	14	1.0250	1.0258	1.0250	1.0250
	θ_B /°	14	-16.7862	-16.7129	-16.7862	-16.7862
	P_B /MW	14	4.1870	3.8022	4.1870	4.1870
	Q_B /MVar	14	2.8673	2.6946	2.8673	2.8673
A2	V_B /p.u.	14	1.0253	1.0258	1.0253	1.0253
	θ_B /°	14	-16.4631	-16.7129	-16.4631	-16.4631
	P_B /MW	14	2.7328	3.8022	2.7328	2.7328
	Q_B /MVar	14	3.3923	2.6946	3.3923	3.3923
A4	V_B /p.u.	14	1.0284	1.0258	1.0284	1.0284
	θ_B /°	14	-16.8432	-16.7129	-16.8432	-16.8432
	P_B /MW	14	4.1749	3.8022	4.1749	4.1749
	Q_B /MVar	14	1.3482	2.6946	1.3482	1.3482
C1	V_B /p.u.	5	1.0084	1.0109	1.0084	1.0084
		11	1.0284	1.0340	1.0284	1.0284
		14	1.0133	1.0184	1.0133	1.0133
	θ_B /°	5	-10.8158	-10.2009	-10.8158	-10.8158
		11	-19.8116	-18.2127	-19.8116	-19.8116
		14	-20.5695	-19.0040	-20.5695	-20.5695
	P_B /MW	5	10.8995	8.5019	10.8995	10.8995
		11	21.1376	15.1057	21.1376	21.1376
		14	8.7928	5.1007	8.7928	8.7928
	Q_B /MVar	5	5.3294	5.1096	5.3294	5.3294
		11	9.6970	8.7284	9.6970	9.6970
		14	3.6529	3.5037	3.6529	3.6529
C3	V_B /p.u.	5	1.0122	1.0109	1.0122	1.0122
		11	1.0252	1.0340	1.0252	1.0252
		14	1.0090	1.0184	1.0090	1.0090
	θ_B /°	5	-11.0737	-10.2009	-11.0737	-11.0737
		11	-17.9815	-18.2127	-17.9815	-17.9815
		14	-19.0012	-19.0040	-19.0012	-19.0012
	P_B /MW	5	28.2841	8.5019	28.2841	28.2841
		11	10.0556	15.1057	10.0556	10.0556
		14	3.7782	5.1007	3.7782	3.7782
	Q_B /MVar	5	-3.4064	5.1096	-3.4064	-3.4064
		11	16.2091	8.7284	16.2091	16.2091
		14	7.5014	3.5037	7.5014	7.5014

for numerical experiments, as shown in Appendix B. The accuracy test is discussed in Subsection A. The convergence and efficiency tests are discussed in Subsection B.

A. Accuracy

The proposed SIAM will be compared with the following three methods in terms of accuracy.

i) NRM based on the global model (NRM-GM): under the global model, TN and DNs will be completely spliced as an entire network. Power flow will be solved with NRM. This method is unrealistic in real-world operation, but the results under this method are accurate, which can be applied as benchmarks.
ii) NRM based on the equivalent model (NRM-EM): under the equivalent model, DNs will be equivalent as constant loads when solving the power flow in the TN, while TN will be equivalent as a constant voltage source when solving the power flow in the DNs. Power flow will be solved with NRM.
iii) MSSM [4]: TN power flow and DN power flow will be both solved with the NRM.

TABLE II
CONVERGENCE AND EFFICIENCY COMPARISON

Case	MSSM-I		MSSM-II		SIAM	
	Iteration Number	Time Cost /ms	Iteration Number	Time Cost /ms	Iteration Number	Time Cost /ms
A1	4	17.3	4	17.6	4	19.8
A2	20	71.8	20	76.1	6	27.3
A3	Diverge		Diverge		8	37.3
A4	9	35.3	9	36.2	6	26.7
A5	45	159.0	45	168.1	8	36.8
B1	4	41.8	4	41.5	4	41.5
B2	19	157.1	19	161.9	4	45.2
B3	Diverge		Diverge		6	63.1
B4	6	58.7	6	61.5	5	55.8
B5	11	95.4	11	99.4	6	65.3
C1	5	35.3	4	29.9	4	33.6
C2	12	64.4	5	32.5	5	36.8
C3	25	99.6	5	23.3	5	33.0
D1	20	789.4	16	657.0	8	332.5
D2	39	1297.4	30	1016.6	12	464.6

Table I compares the power flow results (the voltage of boundary buses and power injections at the boundary) under different methods and different cases. Generally, the NRM-EM cannot achieve accurate power flow solutions because the network losses, DGs, and loops in DNs will all be neglected. The proposed SIAM can achieve the same accuracy to the NRM-GM and the MSSM.

More specifically, comparing the results of Case A1, A2, and A4, the NRM-EM cannot accurately analyze the influences of DGs, while the proposed SIAM, as well as the NRM-GM and the MSSM, can. Compared the results of Case C1 and Case C3, the NRM-EM cannot accurately analyze the influences of loops in DNs, while the proposed SIAM, as well as the NRM-GM and MSSM, can.

B. Convergence and Efficiency

The proposed SIAM will be compared with the following two methods in terms of convergence and efficiency.

i) MSSM-I: the MSSM presented in [2] without the equivalent method for DNs.
ii) MSSM-II: the modified MSSM presented in [4] considering the equivalent method for DNs.

In the whole Section V, note that an iteration of the SIAM means DN power flow and TN power flow are solved once respectively. It is not the iteration from n to $n+1$ implied in (9). Thus, the iteration numbers of the MSSM and the proposed SIAM can be compared directly.

Table II compares the number of iterations and time consumption under different methods and different cases. Generally, the proposed SIAM has the best convergence and highest efficiency among the three methods. It can converge for all the test cases. However, both the MSSM-I and the MSSM-II will diverge for Case A3 and Case B3. Also, for the cases in which all the three methods converge, the SIAM needs the least iterations to achieve the same accuracy.

Compared with Case A1, some PV-typed DGs exist in Case A2 and A3. These DGs significantly increase the sensitivity of reactive power injection to the voltage magnitude at the root

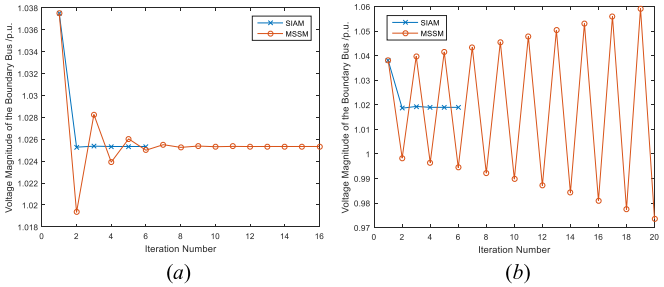

Fig. 4. The variation of the voltage magnitude of the boundary bus.

node. Thus, the MSSM-I suffers from a low convergence rate or even diverges. The MSSM-II is an improvement of the MSSM-I. However, the results show that the MSSM-II does not have a significant improvement in the convergence and efficiency when handling the PV-typed DGs. To be more specific, in the MSSM-II, the equivalent admittance matrix $\boldsymbol{Y}_{eq} \approx 0$ and the MSSM-II is equivalent to the MSSM-I. On the other hand, some DGs with volt-var control exist in Case A4 and A5. Different from PV-typed DGs, the DGs with volt-var control significantly increase the sensitivity of active power injection to the voltage magnitude at the root node. As shown in the table, the MSSM-I and MSSM-II also suffer from a lower convergence rate. Compared with the MSSM-I and MSSM-II, the proposed SIAM can effectively improve convergence when handling DGs with volt-watt and volt-var control modes. The results under Case B1-B5 demonstrate the same point.

Compared with Case C1, some loops exist in the Case C2 and C3. These loops also significantly increase the sensitivity of reactive power injection to the voltage magnitude at the root node. Thus, the MSSM-I needs many more iterations to converge. The MSSM-II effectively improves the convergence of the MSSM-II with the equivalent method. The proposed SIAM has similar convergence and efficiency with the MSSM-II in these cases.

Case D1 and D2 are two large-scale I-T&D cases. There are 16 DNs in each case, including the passive DNs, DNs with DGs, DNs with loops, and DNs with DGs and loops. The proposed SIAM has the best convergence and efficiency. It saves around 2/3 iterations and time compared with the MSSM-I, as well as saves around 1/2 iterations and time compared with the MSSM-II.

Then, a further discussion in Case A2 and A3 is presented. Fig. 4 shows the variation of V_B with the iterations under the SIAM and the MSSM (the MSSM-I and the MSSM-II almost have the same curve since $\boldsymbol{Y}_{eq} \approx 0$). For Case A2, SIAM has a much faster convergence rate than the MSSM, as shown in Fig. 4(a). For Case A3, the MSSM diverges while the SIAM still converges fast, as shown in Fig. 4(b).

Comparing Case A2 and A3, DGs are accessed into different nodes. These DGs are all PV-typed and the voltage magnitude setpoints are all 1.0 p.u. The DGs in Case A3 are accessed into Node 45, 61 which are far away from the root node, which indicates that more reactive power will be outputted from the DGs to maintain the setpoint. Thus, the sensitivity of reactive power injection to the voltage magnitude at the root node is large,

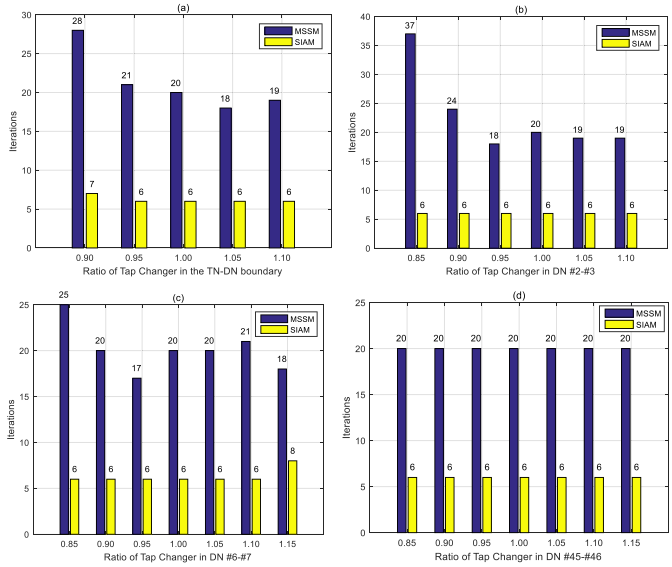

Fig. 5. Iterations under different ratios of tap changers.

which leads to the divergence of the MSSM. On the contrary, the DGs in Case A2 are accessed into Node 8, 15, 20 which are closer to the root node, so the sensitivity is smaller and the MSSM can converge. Fig. 4 shows that the proposed SIAM can enhance the convergence and efficiency in both two cases. The sensitivity of reactive power injection to the voltage magnitude at the root node is not a limiting factor for the convergence and efficiency of the SIAM.

C. Handling On-Load Tap Changers

First, Case A2 is used to test the performance considering the on-load tap changing transformers. Fig. 5 shows the iterations under different ratios of tap changers. A TN-DN boundary transformer is considered in Fig. 5(a). The branches DN #2-#3, DN #6-#7, DN #45-#46 are considered as transformer branches in Fig. 5(b), 5(c), and 5(d), respectively.

As shown in Fig. 5, the performance of the conventional MSSM will be significantly influenced by the ratios of tap changers (the MSSM-I and the MSSM-II almost have the same performance for this case) because the ratios will influence the sensitivity of the reactive power injection to the voltage magnitude at the root node. For example, when the ratio of tap changer in DN #2-#3 is 0.95, the MSSM only takes 18 iterations to converge while it takes 37 iterations when this ratio is 0.85. However, the proposed SIAM can effectively improve the convergence and its performance is more robust and stable to different ratios than the MSSM. The iterations of the SIAM are almost constants under different ratios.

Then, Case A1-A3 are used to test the performance considering the tap changer actions. It is assumed that some branches in these cases are transformer branches and the transformers are equipped with on-load tap changers keeping the voltage of constrained nodes within the interval [0.99, 1.01] p.u. The on-load tap changers adjust the transformer ratios in the range [0.84, 1.16] over 33 positions (thus from one position to the next, the ratio varies by 0.01). The initial position is 1.00.

TABLE III
POWER FLOW RESULTS AND PERFORMANCE COMPARISON CONSIDERING TAP CHANGERS

Case	Tap Changers	Constrained Node	Power Flow Results	MSSM			SIAM		
				Rounds	Total Iterations	Time/ms	Rounds	Total Iterations	Time/ms
A1	-	-	V_B = 1.0250 p.u.; P_B = 4.1870 MW; Q_B = 2.8673 MVar	1	4	17.3	1	4	19.8
	TN-DN boundary	DN #1	V_B = 1.0049 p.u.; P_B = 4.2083 MW; Q_B = 2.8768 MVar	3	12 (=4+4+4)	50.3	3	12 (=4+4+4)	53.9
	DN #2 - #3	DN #3	V_B = 1.0250 p.u.; P_B = 4.2082 MW; Q_B = 2.8768 MVar; $V_{\#3}$ = 1.0044 p.u.	3	10 (=4+3+3)	42.5	3	10 (=4+3+3)	45.7
	TN-DN boundary DN #45 - #46	DN #1 DN #46	V_B = 1.0050 p.u.; P_B = 4.1621 MW; Q_B = 2.8594 MVar; $V_{\#46}$ = 1.0011 p.u.	10	33 (=4+4+4+3+3 +3+3+3+3+3)	146.6	10	33 (=4+4+4+3+3 +3+3+3+3+3)	151.5
A2	-	-	V_B = 1.0253 p.u.; P_B = 2.7328 MW; Q_B = 3.3923 MVar	1	20	71.8	1	6	27.3
	TN-DN boundary	DN #1	V_B = 1.0050 p.u.; P_B = 2.7072 MW; Q_B = -1.0510 MVar	4	74 (=20+18+18+18)	292.6	4	24 (=6+6+6+6)	119.7
	DN #2 - #3	DN #3	V_B = 1.0351 p.u.; P_B = 2.7071 MW; Q_B = -1.0503 MVar; $V_{\#3}$ = 1.0048 p.u.	4	70 (=20+17+17+16)	267.2	4	24 (=6+6+6+6)	116.9
	TN-DN boundary DN #45 - #46	DN #1 DN #46	V_B = 1.0050 p.u.; P_B = 2.6833 MW; Q_B = -1.0180 MVar; $V_{\#46}$ = 0.9908 p.u.	6	92 (=20+18+18 +18+9+9)	355.2	6	32 (=6+6+6+6+4+4)	153.0
A3	-	-	V_B = 1.0190 p.u.; P_B = 3.2087 MW; Q_B = 6.0261 MVar	Diverge			1	8	37.3
	TN-DN boundary	DN #1	V_B = 1.0090 p.u.; P_B = 3.2539 MW; Q_B = 1.4273 MVar				3	20 (=8+6+6)	98.5
	DN #2 - #3	DN #3	V_B = 1.0292 p.u.; P_B = 3.2538 MW; Q_B = 1.4307 MVar; $V_{\#3}$ = 1.0086 p.u.				3	20 (=8+6+6)	98.7
	TN-DN boundary DN #45 - #46	DN #1 DN #46	V_B = 1.0090 p.u.; P_B = 3.2382 MW; Q_B = 1.4440 MVar; $V_{\#46}$ = 0.9964 p.u.				4	24 (=8+6+6+4)	115.3

TABLE IV
PERFORMANCE UNDER GIVEN CONTINGENCIES

Contingency	Alarm	MSSM		SIAM	
		Iteration Number	Time Cost /ms	Iteration Number	Time Cost /ms
Line #6-#13	/	28	101.1	6	19.8
Line #9-#14	Bus #7, #9, #11	Diverge		6	27.4
Line #10-#11	Bus #11	21	78.6	6	27.5
Gen. #6	/	34	122.0	6	27.9

TABLE V
CONTINGENCY ANALYSIS BASED ON DIFFERENT APPROACHES

Case	Total Number of Contingencies	MSSM		SIAM	
		Number of Contingencies which MSSM converges	Time Cost /ms	Number of Contingencies which SIAM converges	Time Cost /ms
A1	23	23	339.7	23	379.8
A2	23	21	1538.9	23	593.6
A3	23	0	5185.4	23	751.7

Table III records the power flow results under different cases. Different tap changer actions will bring out significantly different power flow distribution. Also, this table records the rounds, total iterations, and time consumption of two methods. Here, after a round of power flow calculation, the tap changers will vary by one position according to the voltage magnitudes of constrained nodes. Finally, after the last round, the voltage magnitudes of all constrained nodes should be kept within the allowed interval [0.99, 1.01] p.u. As shown in Table III, different rounds and total iterations are needed when different tap changers are considered. Generally, the MSSM can handle Case A1 and A2 but diverges for Case A3. The proposed SIAM can show satisfying convergence for all cases. Also, it can save around two-thirds of total iterations and time consumptions in Case A2 compared with the MSSM.

D. Application in Contingency Analysis

First, Case A2 is used to test the performance of the MSSM and the SIAM under given contingencies. The alarms of voltage limit violations of PQ-typed buses in the TN will be considered in contingency analysis. As shown in Table IV, different contingencies will significantly influence the convergence of the MSSM. For example, under the contingency of Line #6-#13, the MSSM diverges; under the contingency of Generation #6, the convergence rate of the MSSM is slow and it needs 34 iterations. However, the convergence of the SIAM is very stable, and it needs 6 iterations under all the contingencies presented in Table IV.

Then, Case A1-A3 are used to test the performance of a complete contingency analysis. All N-1 generator contingencies and line contingencies in the TN which will not lead to network splitting are considered. Table V compares the total time consumption and the number of contingencies under which the approaches can converge. The MSSM diverges under two contingencies in Case A2 and all contingencies in Case A3. However, the proposed SIAM can converge under all contingencies in all three cases. Also, it can effectively enhance the overall efficiency of the TN contingency analysis.

VI. CONCLUSION

In this paper, the SIAM is proposed for the power flow calculation of I-T&D. Through extensive demonstration in many cases, the following observations can be obtained:

TABLE VI
TEST CASE INFORMATION

Case	TN Case	DN Case	Closed switches	DGs are accessed into Node No. (Control Mode)	Number of DNs	Number of feeders in each DN	DNs are accessed into Bus No.
A1	case14	case69	radial	-	1	1	(14)
A2	case14	case69A	radial	8, 15, 20 (PV)	1	1	(14)
A3	case14	case69B	radial	45, 61 (PV)	1	1	(14)
A4	case14	case69A	radial	8, 15, 20 (QV)	1	1	(14)
A5	case14	case69B	radial	45, 61 (QV)	1	1	(14)
B1	case57	case69	radial	-	4	1	(8), (9), (12), (18)
B2	case57	case69A	radial	8, 15, 20 (PV)	4	1	(8), (9), (12), (18)
B3	case57	case69B	radial	45, 61 (PV)	4	1	(8), (9), (12), (18)
B4	case57	case69A	radial	8, 15, 20 (QV)	4	1	(8), (9), (12), (18)
B5	case57	case69B	radial	45, 61 (QV)	4	1	(8), (9), (12), (18)
C1	case14	case16	radial	-	1	3	(5, 11, 14)
C2	case14	case16A	5-11	-	1	3	(5, 11, 14)
C3	case14	case16B	5-11, 10-14	-	1	3	(5, 11, 14)
D1	case118	case69	radial	-	4	1	(1), (4), (19), (22)
		case69A	radial	8, 15, 20 (PV)	7	1	(2), (3), (5), (12), (20), (21), (23)
		case16	radial	-	1	3	(24, 25, 26)
		case16A	5-11	-	2	3	(9, 10, 11), (16, 17, 18)
		case16B	5-11, 10-14	-	2	3	(6, 7, 8), (13, 14, 15)
D2	case118	case69	radial	-	4	1	(1), (4), (19), (22)
		case69A	radial	8, 15, 20 (PV)	4	1	(2), (5), (20), (23)
		case69B	radial	45, 61 (PV)	3	1	(3), (12), (21)
		case16	radial	-	1	3	(24, 25, 26)
		case16A	5-11	-	2	3	(9, 10, 11), (16, 17, 18)
		case16B	5-11, 10-14	-	1	3	(6, 7, 8)
		case16C	5-11, 10-14	6, 12, 15 (PV)	1	3	(13, 14, 15)

- The SIAM can achieve the same accuracy to the methods under the global model as well as the MSSM.
- The convergence of SIAM is stable, not sensitive to the effect of DNs on the TN. To be more specific, it can maintain a high convergence rate and efficiency when PV-typed DGs, DGs with volt-var control, on-load tap changing transformers, and loops exist in DNs. Especially when PV-typed DGs exist in DNs, for the cases under which the MSSM can converge, the SIAM takes fewer iterations and less time; for the cases under which the MSSM diverges, the SIAM still converges with a high convergence rate and efficiency.
- In the large-scale complex systems, the SIAM has better performance. It can usually save around 50% iterations and time consumption compared with the MSSM.
- The SIAM can be applied in the TN contingency analysis considering the influences of DNs. It shows more stable convergence under different contingencies and significantly improves the efficiency of the overall contingency analysis compared with the MSSM.

The proposed SIAM can significantly benefit real practice. Future work will extend it to solve other problems related to I-T&D coordinated analysis, such as optimal power flow, economic dispatch, etc.

APPENDIX A

Detailed Formulation of Power Flow of I-T&D

The detailed formulation of the power flow of I-T&D is as follows. First, in the TN part, (1a) can be specified as

$$P_T^i - V_T^i \sum_{j=1}^{n_T} V_T^j (g_T^{ij} \cos\theta_T^{ij} + b_T^{ij} \sin\theta_T^{ij}) - V_T^i \sum_{j=1}^{n_B} V_B^j (g_{TB}^{ij} \cos\theta_{TB}^{ij} + b_{TB}^{ij} \sin\theta_{TB}^{ij}) = 0, i \in S_T \tag{A-1}$$

$$Q_T^i - V_T^i \sum_{j=1}^{n_T} V_T^j (g_T^{ij} \sin\theta_T^{ij} - b_T^{ij} \cos\theta_T^{ij}) - V_T^i \sum_{j=1}^{n_B} V_B^j (g_{TB}^{ij} \sin\theta_{TB}^{ij} - b_{TB}^{ij} \cos\theta_{TB}^{ij}) = 0, i \in S_T \tag{A-2}$$

Then, (1b) and (1c) can be specified as

$$V_B^i \sum_{j=1}^{n_T} V_T^j (g_{TB}^{ij} \cos\theta_{TB}^{ij} + b_{TB}^{ij} \sin\theta_{TB}^{ij}) = P_B^i, i \in S_B \tag{A-3}$$

$$V_B^i \sum_{j=1}^{n_T} V_T^j (g_{TB}^{ij} \sin\theta_{TB}^{ij} - b_{TB}^{ij} \cos\theta_{TB}^{ij}) = Q_B^i, i \in S_B \tag{A-4}$$

Then, in the DN part, (2) can be specified as

$$P_D^i - V_D^i \sum_{j=1}^{n_D} V_D^j (g_D^{ij} \cos\theta_D^{ij} + b_D^{ij} \sin\theta_D^{ij}) - V_D^i \sum_{j=1}^{n_B} V_B^j (g_{BD}^{ij} \cos\theta_{BD}^{ij} + b_{BD}^{ij} \sin\theta_{BD}^{ij}) = 0, i \in S_D \tag{A-5}$$

$$Q_D^i - V_D^i \sum_{j=1}^{n_D} V_D^j (g_D^{ij} \sin\theta_D^{ij} - b_D^{ij} \cos\theta_D^{ij})$$

$$- V_D^i \sum_{j=1}^{n_B} V_B^j (g_{BD}^{ij} \sin\theta_{BD}^{ij} - b_{BD}^{ij} \cos\theta_{BD}^{ij}) = 0, i \in S_D \tag{A-6}$$

where P and Q represent nodal active power and reactive power injection, respectively. θ^{ij} represents the angle difference between Node i and Node j. g and b represent conductance and susceptance. S represents the set of nodes. n represents the number of nodes. The subscripts T, B, and D represent the TN part, boundary part, and DN part, respectively.

Thus, the detailed expressions of intermediate variables shown in (3) are as follows

$$P_B^i = V_B^i \sum_{j=1}^{n_D} V_D^j (g_{BD}^{ij} \cos\theta_{BD}^{ij} + b_{BD}^{ij} \sin\theta_{BD}^{ij}), i \in S_B \tag{A-7}$$

$$Q_B^i = V_B^i \sum_{j=1}^{n_D} V_D^j (g_{BD}^{ij} \sin\theta_{BD}^{ij} - b_{BD}^{ij} \cos\theta_{BD}^{ij}), i \in S_B \tag{A-8}$$

APPENDIX B

Test Case Information

Several I-T&D cases are constructed, as shown in Table VI. The DGs accessed into DNs. When they are considered as PV-typed, they have a constant active power output 0.5MW. When they are controlled with volt-var mode (QV), they have a constant reactive power output 0.5MVar. Each feeder is connected to the TN via a transformer with $r = 0.002$ p.u., $x = 0.01$ p.u., and $ratio = 1$. Here, case69 [15] and case16 [16] are two DN cases. Other DN cases are the modifications to these two cases by closing some switches or accessing some DGs.

REFERENCES

[1] E. Rivero, D. Six, and H. Gerard, "Basic schemes for TSO-DSO coordination and ancillary services provision," *EU Horizon 2020 Smart-Net Project*, Dec. 2016. [Online]. Available: https://smartgrids.no/ wp-content/uploads/sites/4/2016/01/ISGAN-TSO-DSO- interaction.pdf

[2] H. Sun, Q. Guo, B. Zhang, Y. Guo, Z. Li, and J. Wang, "Master–slave-splitting based distributed global power flow method for integrated transmission and distribution analysis," *IEEE Trans. Smart Grid*, vol. 6, no. 3, pp. 1484–1492, May 2015.

[3] Q. Huang and V. Vittal, "Integrated transmission and distribution system power flow and dynamic simulation using mixed three-sequence/three-phase modeling," *IEEE Trans. Power Syst.*, vol. 32, no. 5, pp. 3704–3714, Sep. 2017.

[4] K. Li, X. Han, W. Li, and R. Ahmed, "Unified power flow algorithm of transmission and distribution network," in *Proc. IEEE 6th Int. Conf. Renewable Energy Res. Appl.*, San Diego, CA, 2017, pp. 257–261.

[5] Z. Li, H. Sun, Q. Guo, J. Wang, and G. Liu, "Generalized master–slave-splitting method and application to transmission–distribution coordinated energy management," *IEEE Trans. Power Syst.*, vol. 34, no. 6, pp. 5169–5183, Nov. 2019.

[6] Z. Li, Q. Guo, H. Sun, and J. Wang, "Coordinated economic dispatch of coupled transmission and distribution systems using heterogeneous decomposition," *IEEE Trans. Power Syst.*, vol. 31, no. 6, pp. 4817–4830, Nov. 2016.

[7] Z. Li, Q. Guo, H. Sun, and J. Wang, "Coordinated transmission and distribution AC optimal power flow," *IEEE Trans. Smart Grid*, vol. 9, no. 2, pp. 1228–1240, Mar. 2018.

[8] J. Yu, Z. Li, Y. Guo, and H. Sun, "Decentralized chance-constrained economic dispatch for integrated transmission-district energy systems," *IEEE Trans. Power Syst.*, vol. 10, no. 6, pp. 6724–6734, Nov. 2019.

[9] Z. Li, Q. Guo, H. Sun, J. Wang, Y. Xu, and M. Fan, "A distributed transmission-distribution-coupled static voltage stability assessment method considering distributed generation," *IEEE Trans. Power Syst.*, vol. 33, no. 3, pp. 2621–2632, May 2018.

[10] J. Zhao, H. Wang, Y. Liu, Q. Wu, Z. Wang, and Y. Liu, "Coordinated restoration of transmission and distribution system using decentralized scheme," *IEEE Trans. Power Syst.*, vol. 34, no. 5, pp. 3428–3442, Sep. 2019.

[11] R. Roofegari nejad, W. Sun, and A. Golshani, "Distributed restoration for integrated transmission and distribution systems with DERs," *IEEE Trans. Power Syst.*, vol. 34, no. 6, pp. 4964–4973, Nov. 2019.

[12] Z. Li, J. Wang, H. Sun, and Q. Guo, "Transmission contingency analysis based on integrated transmission and distribution power flow in smart grid," *IEEE Trans. Power Syst.*, vol. 30, no. 6, pp. 3356–3367, Nov. 2015.

[13] Z. Li, J. Wang, H. Sun, and Q. Guo, "Transmission contingency screening considering impacts of distribution grids," *IEEE Trans. Power Syst.*, vol. 31, no. 2, pp. 1659–1660, Mar. 2016.

[14] Z. Li, *Distributed Transmission-Distribution Coordinated Energy Management Based on Generalized Master-Slave Splitting Theory*, 1st ed., Singapore: Springer, 2018.

[15] D. Das, "Optimal placement of capacitors in radial distribution system using a fuzzy-GA method," *Int. J. Electr. Power Energy Syst.*, vol. 30, no. 6, pp. 361–367, Jul. 2008.

[16] S. Civanlar, J. J. Graiger, H. Yin, and S. S. H. Lee, "Distribution feeder reconfiguration for loss reduction," *IEEE Trans. Power Del.*, vol. 3, no. 3, pp. 1217–1223, Jul. 1988.

Kunjie Tang (Student Member, IEEE) received the B.E degree from the College of Electrical Engineering, Zhejiang University, Hangzhou, China, in 2017, where he is currently pursuing the Ph.D. degree. His research interests include transmission-distribution coordinated optimization and high-performance computing in power systems.

Shufeng Dong received the B.E. and Ph.D. degrees from the Department of Electrical Engineering, Tsinghua University, Beijing China, in 2004 and 2009, respectively. Currently, he is an Assistant Professor and Qiushi Young Scholar with College of Electrical Engineering, Zhejiang University. His research interests include power system state estimation, cloud computing, and high-performance computing in power systems.

Yonghua Song (Fellow, IEEE) received his B.Eng. and Ph.D. from the Chengdu University of Science and Technology (now Sichuan University) and China Electric Power Research Institute in 1984 and 1989 respectively. He is currently the Rector of University of Macau and the Director of State Key Laboratory of Internet of Things for Smart City, and also an Adjunct Professor with the Department of Electrical Engineering, Tsinghua University, and the College of Electrical Engineering, Zhejiang University. He was awarded DSc, Honorary DEng and Honorary DSc by Brunel University, University of Bath and University of Edinburgh. He is a Fellow of the Royal Academy of Engineering and a Foreign Member of Academia Europaea.